Neural Networks as Valuable Tools To Differentiate between Sesquiterpene Lactones' Inhibitory Activity on Serotonin Release and on NF-κB

Steffen Wagner,[†] Raul Arce,[‡] Renato Murillo,[‡] Lothar Terfloth,[§] Johann Gasteiger,[§] and Irmgard Merfort*[,†]

Institut für Pharmazeutische Wissenschaften, Lehrstuhl für Pharmazeutische Biologie and Biotechnologie, Universität Freiburg, 79104 Freiburg, Germany, Escuela de Quimica y Centro de Investigación en Productos Naturales (CIPRONA), Universidad de Costa Rica, San José, Costa Rica, and Molecular Networks GmbH−Computerchemie, 91052 Erlangen, Germany

Received October 19, 2007

Sesquiterpene lactones are the active components of a variety of medicinal plants from the Asteraceae familiy. They possess biological activities such as the inhibition of NF-κB and the release inhibition of the vasoactive serotonin. On the basis of a data set of 54 SLs, we report the development of a quantitative model for the prediction of serotonin release inhibition. Comparing this model with a previous investigation of the target NF-κB, structural features necessary for specific compounds could be acquired. Atomic properties encoded by radial distribution function and molecular surface potentials encoded by autocorrelation were used as descriptors. Whereas some descriptors describe the structural requirements for both activities, other descriptors can be used to decide whether an SL is more active to NF-κB or to serotonin release. Again, counter propagation neural networks proved to be a valuable tool to establish structure–activity relationships that are necessary for the search for and optimization of lead structures.

Introduction

Sesquiterpene lactones (SLs)[a] belong to one of the largest groups of secondary plant metabolites and are the active components of many medicinal plants from the Asteraceae family. They possess a wide variety of biological activities[1,2] such as the inhibition of the central transcription factor NF-κB[3–5] and the inhibition of the release of the vasoactive serotonin.[6] NF-κB is a central regulator of many genes involved in immunological responses. Because of this pivotal role, NF-κB and the signaling pathways that regulate its activity have become a focal point for intense drug discovery.[7–11] We have recently reported that SLs can serve as leads for the development of potent NF-κB inhibitors and that a counterpropagation neural network (CPGNN) can serve as a valuable tool for selecting these leads.[12] Our investigation strengthened the importance of the α,β-unsaturated carbonyl structures and the hydrogen binding potential (HBP) projected on the surface for the NF-κB inihibitory activity.

Serotonin (5-hydroxytryptamine, 5-HT) is believed to play roles both as a vasoactive agent and neurotransmitter in the etiology of migraine.[6,13] Preparations of *Tanacetum parthenium* (L.) Schultz Bip., the so-called feverfew, have been clinically proven to reduce the incidence and severity of migraine headaches.[13,14] The SL parthenolide is discussed as its main active secondary metabolite, as it inhibits the release of serotonin in bovine platelets.[15] Serotonin release was also inhibited by helenalin in human platelets.[16] Previously, a SAR study including 54 structurally different SLs was undertaken on the same topic.[6] It was found that total hydrophobicity and steric bulk do not correlate well with the inhibitory activity on serotonin release but that steric bulk and electrostatic potential at particular points on the skeleton affect the activity.

As a common molecular mechanism, the reaction of the exomethylene group of the γ-lactone ring with nucleophiles, especially with the sulfhydryl group of cysteine, in a Michael-type addition is discussed.[17] This could be shown for helenalin by alkylation of cysteine 38 in the p65/NF-κB subunit.[3,18] Because of the reactive α,β-unsaturated carbonyl structures present in SLs, they have often been considered as unspecific substances that launch a "sweeping attack" on all possible targets without any specificity, a property contradictory for any drug development. The question arises if selection of SLs with specific activities is possible. Here we demonstrate that CPGNN can be used to solve this necessary task.

CPGNN is an artificial neural network (ANN). These computational models are based on the simplified concept of the brain, in which nodes, called neurons, are interconnected in a network-like structure.[19] Self-organizing networks, introduced by Kohonen in the 1980s, project objects from a multidimensional space into a lower-dimensionality space, usually into a 2D plane.[20,21] Thereby, the topology of the input space is preserved in the projection. Counterpropagation networks utilize the Kohonen algorithm but consider the investigated property during the training process. Because high-dimensional values of a 3D structure representation shall be used as descriptors, CPGNN is a suitable option.[22]

On the basis of the above-mentioned data set of 54 SLs,[6] we report the development of a QSAR model to predict the serotonin release inhibitiory activity based on CPGNN. This data set includes SLs of four different skeletal types: 18 germacranolides, 17 eudesmanolides, 8 guaianolides, and 11 pseudoguaianolides exhibiting IC_{50} values between 1.78 and >624.2 μM (Figure 6, Table 7). Comparison of this model with a previous investigation that produced a structural model for

* To whom correspondence should be addressed. Phone: +49-761-2038373. Fax: +49-761-2038383. E-mail: irmgard.merfort@pharmazie.uni-freiburg.de.

[†] Universität Freiburg.

[‡] Universidad de Costa Rica.

[§] Molecular Networks GmbH−Computerchemie.

[a] Abbreviations: SL, sesquiterpene lactones; ANN, artificial neural network; CPGNN, counterpropagation neural network; HBP, hydrogen binding potential; RDF, radial distribution function; AC, autocorrelation; MEP, molecular electrostatic potential; mmPol, mean molecular polarizability; TPSA, topological polar surface area; χ_π, atom-π-electronegativity; χ_σ, atom-σ-electronegativity; α_d, effective atom polarizability; q_σ, atom-σ-charge

10.1021/jm701318x CCC: $40.75
Published on Web 02/14/2008

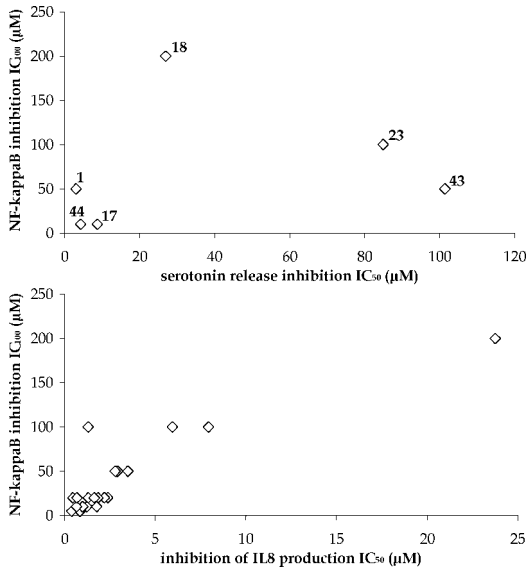

Figure 1. Correlation between inhibition of NF-κB[12] and serotonin release[6] using 6 SLs (top) and inhibition of IL-8[23] production using 23 SLs (bottom).

Table 1. Global Molecular and Atom Properties and Surfaces Used[a]

symbol	description	dimensionality after reduction
log *P*	octanol–water partition coefficient	1[b]
Log *s*	aqueous solubility	1[b]
mmPOL	**mean molecular polarizability**	**1**[b]
TPSA	**topological polar surface area**	**1**[b]
α_d	**effective atom polarizability**	**15**[c]
χ_{LP}	lone pair electronegativity	11[c]
χ_π	**π-electronegativity**	**12**[c]
χ_σ	**σ-electronegativity**	**13**[c]
q_π	π-charge	10[c]
q_σ	**σ-charge**	**12**[c]
q_{tot}	total charge	11[c]
MEP	**electrostatic potential on the molecular surface**	**7**[d]
HBP	**hydrogen binding potential on the molecular surface**	**8**[d]
HPP	hydrophobicity potential on the molecular surface	6[d]

[a] All descriptors were calculated by ADRIANA.Code.[24] The properties in bold show a clustering with a low number of conflicts and a sufficient high occupancy. [b] Global molecular property, no reduction necessary. [c] Atom property, RDF encoded. [d] Molecular surface property, AC-encoded.

the NF-κB activity of SLs[12] allows the specification of structural features necessary for either serotonin or NF-κB activity.

Results and Discussion

Correlation of Inhibitory Activity of SLs on NF-κB and Serotonin Release. To gain first insights into the specificity of SLs, six of these natural compounds that were part of the data set from the NF-κB QSAR study[12] as well as of the data set from the serotonin release QSAR study[6] were chosen and the respective activity was compared. No correlation between these two activities could be observed (Figure 1; correlation coefficient of $R^2 = 0.04$ for linear regression, $n = 6$). Although the overlapping of the two data sets is poor, this is a first clue for a certain specificity of the SLs for the two targets. In contrast, inhibition of NF-κB activity and IL-8 production[23] showed a fairly good correlation (Figure 1; $R^2 = 0.79$; $n = 23$) indicating that NF-κB is involved in IL-8 biosynthesis. When serotonin release inhibition and cytotoxicity were correlated in a former study, no correlation was observed.[6]

Generation of a Counterpropagation Neural Network. The 54 SLs of the data set comprising compounds with IC_{50} values between 1.78 and >624.2 μM were grouped into six activity classes as described in Experimental Section. Properties were calculated for each SL including four global molecular properties, seven atomic properties encoded by radial distribution function (RDF), and three surface potentials encoded by autocorrelation (AC) (Table 1). The global properties mean molecular polarizability (mmPOL) and topological polar surface area (TPSA) show a good correlation of the normalized descriptor with the activity classes and were used for further combinations of vectorial descriptors. The vectors of the atomic properties and of surface potentials were reduced from 128 to between 6 and 15 descriptors (see Experimental Section; Table 1). Four (χ_π, χ_σ, α_d, q_σ) of the seven RDF-coded atomic properties as well as the AC-coded surfaces MEP and HBP show a good clustering with satisfying parameters (conflicts < 21%, occupancy > 77.5%, wrongly clustered neurons < 24.5%). Two vectors of the selected eight properties (mmPOL, TPSA, χ_π, χ_σ, α_d, q_σ, MEP, HBP) were combined with each other, resulting in 28 combinations from which five ($\chi_\pi + \chi_\sigma$, χ_π + HBP, χ_π + MEP, $\chi_\pi + \alpha_d$, $\chi_\pi + q_\sigma$) exhibited a good clustering (conflicts < 12%, occupancy > 81%, wrongly clustered neurons < 22% in at least two categories). In a final step, the five combinations were again combined with the selected eight vectors. From these 20 new combinations two (χ_π + MEP + q_σ, $\chi_\pi + q_\sigma$ + TPSA) show a good clustering.

From the resulting seven best combinations, the one that includes χ_π + MEP + q_σ exhibited good values in the quality categories of clustering, conflicts. and occupancy (Table 2). The exact composition is given in Table 3; an example of a CPGNN

Table 2. Data Characterizing the Best Combinations Using the Kohonen Neural Network[a]

combination	wrongly clustered neurons (%)	occupancy (%)	conflicts (%)
$\chi_\pi + \chi_\sigma$	21.0	79.5	10.2
χ_π + HBP	23.0	**84.5**	**8.3**
χ_π + MEP	22.0	**80.5**	**6.5**
$\chi_\pi + \alpha_d$	**18.5**	78.0	11.1
$\chi_\pi + q_\sigma$	**18.5**	**82.5**	13.0
χ_π + MEP + q_σ	**20.0**	**82.0**	**7.9**
$\chi_\pi + \alpha_d$ + TPSA	**14.0**	77.0	**9.7**

[a] The values are the average of four trainings. The four best values of each category are in bold letters.

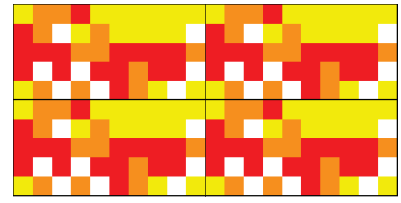

Figure 2. Output map of a toroidal CPGNN with a 1-dimensional output layer of the best model χ_π + MEP + q_σ. High inhibitory activity (activity class 1 and 2) is red, activity classes 3 and 4 are orange, and activity classes 5 and 6 are yellow. The white areas indicate empty neurons. To illustrate the clustering of the different classes, four toroidal maps were arranged like tiles to indicate the closed nature of a toroidal surface.

Table 3. Descriptors of the Best Model Using CPGNN

property	distances (Å)
χ_π	1.4; 1.5; 2.3; 3.0; 3.7; 4.4; 4.5; 4.6; 4.7; 5.4; 6.0; 6.2
MEP	0.2; 2.6; 3.3; 3.9; 4.4; 7.5; 9.2
q_σ	1.2; 1.4; 1.5; 1.7; 1.8; 2.3; 2.6; 3.0; 3.1; 4.7; 7.5; 10.8

Table 4. Confusion Matrix Based on a 10-Fold Cross-Validation of the Best Model χ_π + MEP + q_σ using CPGNN[c]

predicted activity class (PAC)	experimental activity class (EAC) 1	2	3	4	5	6	n_{false} of the PAC[a]
1	2	1	1	1	0	0	2
2	3	5	6	0	0	0	0
3	0	5	2	0	0	0	0
4	1	0	0	0	2	1	2
5	0	0	0	2	3	4	0
6	1	0	0	3	6	5	4
n_{false} of the EAC[b]	2	0	1	4	0	1	8

[a] PAC, predicted activity class. [b] EAC, experimental activity class. [c] n_{false} is the number of wrongly predicted SLs.

Table 5. Wrongly Predicted SLs by Validation

SL	activity class: experimental	activity class: predicted	SLs involved in conflict neurons
1	1	6	**33**
4	4	6	**34**
18	3	1	**1**
23	4	6	**32**
32	6	4	**33**
33	4	6	**32**
44	1	4	**47**
47	4	1	**44**

output map is shown in Figure 2. The SLs with the lowest activity values (activity classes 5 and 6) build an extended cluster. Only one neuron with low activity is not included in this extended cluster, and it is well separated from the other activity classes. The highly active SLs (activity classes 1 and 2) form a band across the whole map that is interrupted only by two empty neurons. The SLs with intermediate activities (activity classes 3 and 4) do not build an isolated cluster; they encircle the neurons of the highly active SLs.

Evaluation of the Best CPGNN. An internal validation by 10-fold cross-validation revealed that a correct prediction of the serotonin release inhibition was possible with 85.2% accuracy (Table 4). The eight wrongly predicted SLs are summarized in Table 5. The SLs **32** and **33** as well as **44** and **47** are pairs that predict each other. Interestingly, a wrong prediction of SLs **1** and **23** is also connected with the predicitions for the SLs **32** and **33**.

Structural Information of Descriptors Used for Serotonin Release Inhibition. The best model includes descriptors based on π-electronegativity (χ_π) and σ-charge (q_σ) of the atoms and on the MEP projected onto the surface (Table 3). Interestingly, χ_π is present in each combination selected during the search for the best model. For the atomic property χ_π high values of the RDF code are associated with a high serotonin release inhibition. The RDF vector of χ_π has values greater than 0 only for atoms with π-electrons, i.e., atoms in multiple bonds and atoms with free electron pairs. Distances of 1.4 and 1.5 Å occur with atoms that are singly bonded to atoms with positive values for χ_π. Such substructures can be found, for example, in the lactone ring with an exomethylene group. Atoms connected by a double bond are not contained in this structural feature because they possess shorter distances of about 1.2 Å. The distance of 2.3 Å is found

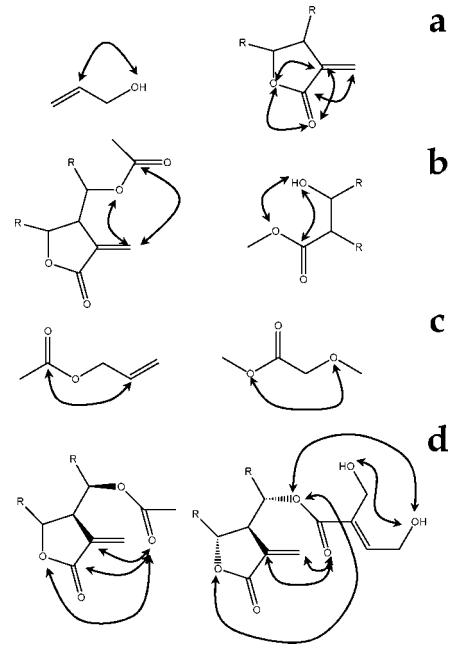

Figure 3. Typical SL structure elements with atomic distances of (a) 2.3, (b) 3.0, (c) 3.7, and (d) 4.4−4.7 Å. The arrows show distances with RDF values of χ_π different from zero. R's in some structure elements are connected and build a six-membered or larger ring.

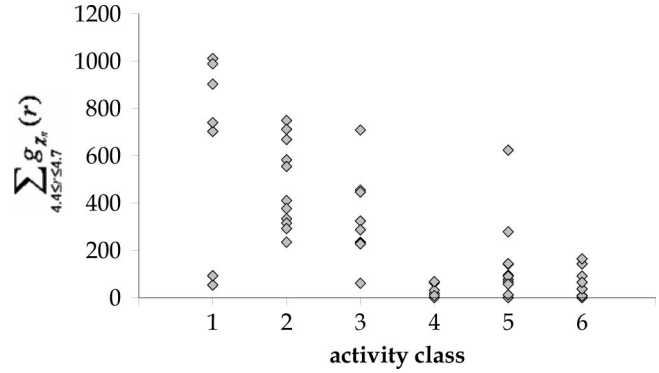

Figure 4. Distribution of the sum of the RDF-encoded property χ_π at atomic distances of 4.4−4.7 Å within the activity classes 1−6. Based on a value of 200, an almost complete differentiation between activity classes 1−3 and 4−6 is possible. Only 3 of 27 SLs (11.1%) of activity classes 1−3 and 2 of 27 SLs (7.4%) of activity classes 3−6 would be falsely classified using the sum of these four RDF values as a descriptor.

between atoms separated by two bonds (Figure 3a). A distance of 3.0 Å is found between atoms separated by three bonds if these atoms are brought together, for example, by incorporation into rings (Figure 3b). A distance of 3.7 Å occurs between atoms separated by three bonds if these are contained in open chain sequences (Figure 3c). The distance of 2.3 Å is mostly found within γ-lactone rings, whereas distances of 3.0 and 3.7 Å occur in structure elements, which do not comprise α,β-unsaturated structures (Figure 3). It is noteworthy that four distances in the range of 4.4−4.7 Å are included in the best model. All of these distances mostly appear between hydroxy, carboxy, and ester groups adjacent to the exomethylene group of the lactone ring on one side and atoms of the γ-lactone ring on the other side (Figure 3d). Whereas the individual atom distances between 4.4 and 4.7 Å exhibit only a marginal correlation of high RDF values

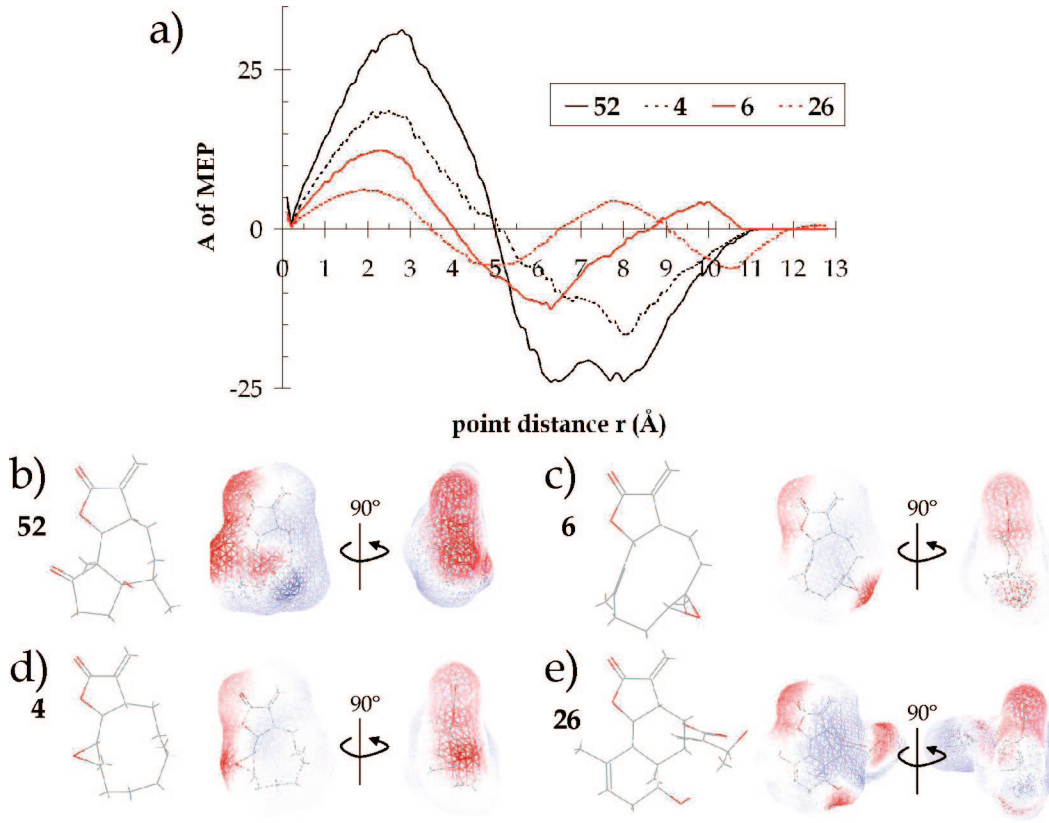

Figure 5. MEP projected onto the surface (b−e) and the corresponding AC curves (a) of four different SLs.

Table 6. Estimation of the Power of Two CPGNN Models for Prediction of NF-κB Inhibitory Activity and for Serotonin Release Inhibition of SLs (%)[a]

	data set			
CPGNN model	NF-κB		serotonin	
NF-κB	occupancy **80.0** wrongly clustered **18.0**	conflicts **5.0** correct predicted **80.6**	occupancy **86.0** wrongly clustered **30.0**	conflicts **16.0** correct predicted **64.8**
serotonin	occupancy **52.5** wrongly clustered **30.9**	conflicts **50.4** correct predicted **71.8**	occupancy **82.0** wrongly clustered **20.0**	conflicts **7.9** correct predicted **85.2**

[a] CPGNN model serotonin is the best model evaluated in this paper; CPGNN model NF-κB was developed in Wagner et al.[12] The estimation include occupancy, conflicts, wrongly clustered neurons and correct predicted SLs. The values demonstrate that the NF-κB model is not suitable for the use of the serotonin release activity and vice versa.

and high serotonin release inhibitory activity, a high correlation can be observed for the sum of these four RDF values:

$$\sum_{4.4 \le r \le 4.7} g_{x_\pi}(r)$$

and the inhibitory activity (Figure 4). The SLs **1** and **44**, which show unusual low values of

$$\sum_{4.4 \le r \le 4.7} g_{x_\pi}(r)$$

for activity class 1, are also wrongly predicted during the validation (Table 5). This demonstrates the significance of the four descriptors for a correct classfication.

Twelve distances from the RDF-encoded atom property q_σ were included in our model. The q_σ values of an atom depend on the atom type, the hybridization, and the neighboring atoms. Oxygen atoms in the SLs of our data set show values between −0.25 and −0.39 e. Hydrogen atoms possess positive values lower than 0.08 e, but hydrogen atoms have values of about 0.21 e in hydroxyl groups and values of about 0.11 e in aldehyde groups. Carbonyl atoms in carbonyl, ester, and hydroxyl groups show positive values of up to +0.30 e; other carbonyl atoms have values between −0.08 and +0.02 e. Active SLs can be characterized by both highly positive or highly negative RDF values depending on the considered distances. With the atom distances of 1.2, 1.4, and 1.5 Å, strongly negative values correlate with a high activity. As mentioned above, a distance of 1.2 Å describes the distance of two atoms connected by double bonds. Considering the q_π values, numerous C=O double bonds (e.g., ketone, aldehyde, ester, lactone) seems to be associated with a high activity. Strongly negative RDF values of the distances of 1.4 and 1.5 Å, which were also used by the atomic property χ_π, can be found within numerous functional groups, such as in lactones, acids, esters, etc. A correlation between high RDF values and high activity can be observed with the distances of 1.7 and 1.8 Å, as well as for a distance of 2.3 Å. The values of 1.7 and 1.8 Å are the distances between geminal bonded hydrogen atoms. High q_σ charges and therefore high positive RDF values are shown for hydrogen atoms bonded to sp^2-hybridized carbon atoms, such as in the exomethylene group of the γ-lactone. The same behavior is shown by carbon atoms with strongly electronegative groups, such as with oxygen or chlorine atoms. As described above (Figure 3a), distances

Table 7. List of Investigated SLs, Their Serotonin Release Inhibitory Activity, and Their Activity Class[6]

no.	name	IC_{50} (μM)	activity class
	I. Germacranolides		
1	parthenolide	3.03	1
2	11β,13-dihydro-parthenolide	>399.5	6
3	1,10-epoxy-11β,13-dihydro-parthenolide	>413.0	6
4	1,10-dihydro-parthenolide	40.58	4
5	stizolicin	5.82	2
6	1,10-epoxy-costunolide	121.3	5
7	ursiniolide A	1.78	1
8	ursiniolide B	5.30	2
9	salonitenolide	10.15	3
10	cnicin	3.52	1
11	alatolide	5.77	2
12	glaucolide A	20.92	3
13	cinerenin	3.52	1
14	cinerenin acetate	2.04	1
15	Schkuhriolide	277.7	5
16	melampodin A	4.68	1
17	enhydrin	8.76	2
18	tatridin B	26.97	3
	II. Eudesmanolides		
19	reynosin	271.1	5
20	11β,13-dihydro-reynosin	>209.7	5
21	reynosin-8β-*O*-epoxyangelate	10.12	3
22	reynosin-8β-*O*-2,3-dihydro-2-methylbutyrate	9.52	2
23	santamarin	84.93	4
24	11β,13-dihydro-santamarin	>199.7	5
25	santamarin-8β-*O*-epoxyangelate	7.09	2
26	santamarin-8β-*O*-(2-hydroxyethyl)-acrylate	26.73	3
27	3,4-*cis*-α-epoxy-8β-epoxyangeloyloxy-santamarin	17.73	3
28	1β-hydroxy-8β-epoxyangeloyloxy-arbusculin B	6.66	2
29	α-santonin	>568.4	6
30	vachanic acid	>614.2	6
31	vachanic acid methylester	201.2	5
32	*iso*-alantolacton	>516.2	6
33	asperilin	57.62	4
34	pulchellin C	>416.2	6
35	telekin	>563.8	6
	III. Guaianolides		
36	grossheimin	22.18	3
37	3-oxo-grandolide	>454.0	6
38	8-*epi*-*iso*-lippidiol	>488.1	6
39	15-deoxy-repin	6.32	2
40	repin	9.24	2
41	centaurepensin	6.06	2
42	artecanin	>134.7	5
43	xerantholide	101.4	5
	IV. Pseudoguaianolides		
44	helenalin	4.28	1
45	linifolin A	11.44	3
46	tenulin	361.3	6
47	6α-hydroxy-2,3-dihydro-aromaticin	60.08	4
48	geigerinin	73.43	4
49	burrodin	251.4	5
50	inuchinenolide C	33.47	3
51	parthenin	129.3	5
52	coronopilin	248.9	5
53	confertiflorin	8.88	2
54	psilostachyin A	44.06	4

of 2.3 Å are found within lactones, ester, and carboxyl groups. Thereby, only the product of the q_σ values of both oxygen atoms contributes to the positive RDF value. All other distances yield negative or small positive values. Similar to the χ_π descriptors, a distance of 3.0 Å was also used within the q_π descriptors. Additionally, a distance of 3.1 Å was added. Some active substances show highly positive values. The same structure elements as within the χ_π descriptors at 3.0 Å contribute to the RDF value, but not all distances result in positive RDF values because q_π charges can have positive or negative values. The same observation can be made for the distance of 4.7 Å, which is also used by the χ_π descriptors. The used distance of 10.8 Å seems to be a standard measure for the size of the molecules. No inactive substance (activity class 4−6) shows an RDF value different from zero and 0.70 after normalization, respectively, whereas 67% of the active compounds (activity class 1−3) show values different from zero and 0.70 after normalization, respectively, which means that the maximal extension of the molecule is not smaller than 10.8 Å. This is only possible if space-filling side chains are present in the molecule.

Seven distances of the AC-encoded MEP projected onto the surface are part of the best model. The calculation of the potential of one surface point is based on the summation of σ charges of the surrounded atoms regarding the distance between atom and surface points. Therefore, positive and negative values are possible for the σ values as well as for the AC-encoded values. Some typical AC curves are presented in Figure 5a. Positive values dominate up to a distance of 3.5−5 Å, followed by a range of negative AC values. For higher distances the values of the AC of the MEP tend to go to zero, in a few cases even giving slightly positive values again. How often the curve changes between positive and negative values depends on the number of continuous areas with positive and negative MEP. If only one area exists with a negative potential, the AC value is typically positive for a distance up to 5 Å, because pairs of points with potentials of the same algebraic sign are dominant up to this distance. For higher distances, pairs of points with potentials of different algebraic signs are dominant. The AC curves show higher positive and negative values, if the surface area with negative potential is larger (Figure 5b and d). If a substance possesses two or more surface areas with a negative potential, additional positive and/or negative amplitudes of the AC curve are monitored (Figure 5b, c, and e). A correlation of low AC values and of high activity can be observed with distances of 0.2, 2.6, 3.3, 3.9, and 4.4 Å. Because adjoining points were regarded at a distance of 0.2 Å, this distance is a measure for the size of the molecule and for the length of the border between positive and negative surface potentials: the longer the border, the lower the AC values. Low AC values occur for the distances 2.6−4.4 Å if the first positive part of the AC curve is narrow and soon pass over to negative values. As already mentioned, therefore a few small separated areas with negative potentials are necessary. Consequently, a high activity correlates with structures having several functional groups containing oxygen atoms. In contrast to the distances mentioned above, high AC values correlate with a high activity at the distances of 7.5 and 9.2 Å. The AC values are high, if the AC curve passes over the zero line two or three times, that is, if several well-separated groups with oxygen atoms are present (Figure 5).

Differences and Similarities of Structural Features Essential for High Activities. The best model for the prediction of the serotonin release inhibitory activity includes descriptors based on the atomic properties χ_π and q_σ, as well as on the MEP. Remarkably, the atomic property χ_π was also used in a model for the NF-κB inhibitory activity of SLs, sometimes even with the same distance. Furthermore, the NF-κB model includes the surface potential HBP.[12]

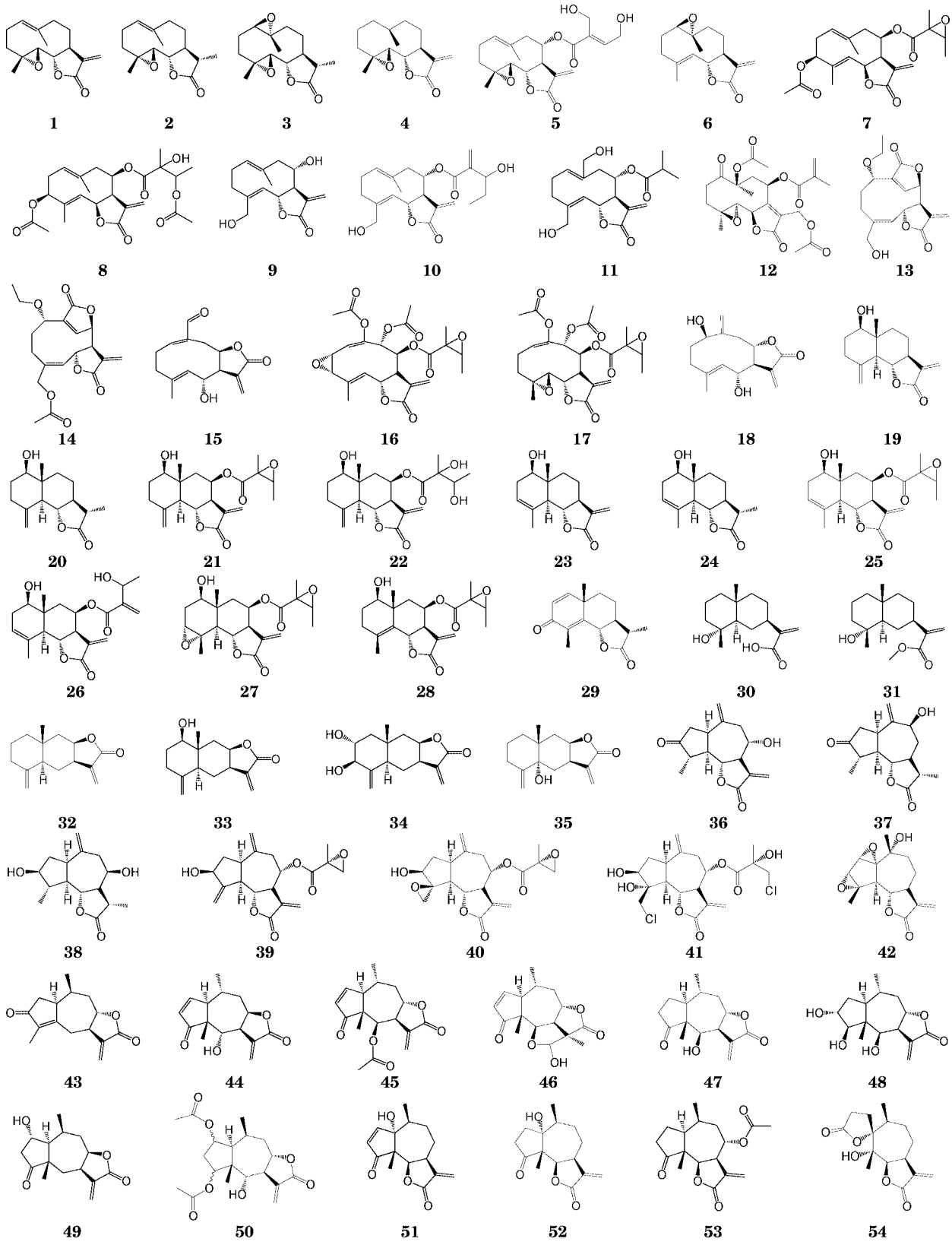

Figure 6. Structures of the investigated sesquiterpene lactones representing four structural classes: gemacranolides (**1**–**18**), eudesmanolides (**19**–**35**), guaianolides (**36**–**43**), and pseudoguaianolides (**44**–**54**).

To test whether the descriptors of both models can be exchanged with each other, the descriptors used in the NF-κB models were calculated for the serotonin data set. Whether these descriptors can be used for the prediction of the serotonin release inhibition was checked in two different ways. At first, a 10-fold cross validation was performed. Furthermore, the usability was estimated by considering conflicts, clustering, and output maps. The same procedure was done vice versa: the descriptors of the serotonin models were used for the NF-κB data set to predict the NF-κB inhibitory activity. Both experiments show

that the descriptors of one model perform poorly in predicting the other activity (Table 6). This may be a further clue for a certain specificity of SLs.

Interestingly the descriptors based on the distances of 1.4 and 1.5 Å of χ_π were used in both models, in addition to the 2.3 Å distance in the serotonin and the 3.5 Å distance in the NF-κB model. The distances 1.4, 1.5, and 2.3 Å of q_σ were also used in the serotonin model. All of these descriptors point to the involvement of a γ-lactone moiety with an exomethylene group, which is known to be essential but not sufficient for a high activity in both targets.[6,15–17,25] This structural element can react with sulfhydryl groups, for example, in cysteine residues by a Michael addition. Accordingly, evidence had been provided that cysteine-38 of the NF-κB subunit p65 is alkylated by helenalin.[3,5] Similar reactions are also discussed for the molecular mechanism of serotonin release inhibition, although the exact molecular target is yet unknown.[6,14] Thus, Luo et al.[26] selected 39 SLs from the serotonin data set of Marles et al.[6] and used descriptors based on HOMO and LUMO in their QSAR study. Thereby, they provided evidence that a reaction between SLs and the unknown target may be involved in the serotonin release inhibition.

Moreover, the distances of 4.4 and 4.5 Å of χ_π are part of both models. In addition to the distances of 4.6 and 4.7 Å of χ_π and 4.7 Å of q_σ used in the serotonin model, these descriptors describe the occurrence of hydroxy, carboxy, and ester groups adjacent to the exomethylene group of the γ-lactone. These functional groups are already known to be important for NF-κB inhibitory activity[25] but yet not for the serotonin release inhibition. The q_σ descriptor at an atom distance of 10.8 Å used in the serotonin model can also be discussed in this context. It describes the presence of space-filling side chains that are only present near the exomethylene group of the γ-lactone in our data set. In summary, an intact γ-lactone with an exomethylene group and an oxygen group adjacent to this exomethylene group are essential structural features for both targets.

Besides the γ-lactone system, further α,β-unsaturated structural features are common in SLs. Whereas the NF-κB model includes atom distances of the RDF-encoded χ_π that can be found within α,β-unsaturated structures (e.g., 2.6, 3.5 Å),[2,25] the serotonin model does not use these descriptors. Interestingly, some SLs not having additional α,β-unsaturated systems (e.g., **7**, **10**, **39**, **53**) show a high serotonin release inhibition. Marles et. al[6] point out that further α,β-unsaturated systems may only contribute to serotonin activity but may not have a strong impact on this activity. In contrast, no SL shows a high NF-κB activity without such a feature.[12,25] Furthermore, the presence of α,β-unsaturated systems, regardless of lactone or cyclopentenone, is responsible for the cytotoxicity of SLs[2,27] and can explain the missing correlation between serotonin release inhibition and cytotoxicity.[6] In summary, it can be assumed that these structural elements are not necessary for high serotonin release inhibition but are needed for high NF-κB inhibition activity.

Both models contain descriptors of an autocorrelation encoded surface potential. Whereas in the serotonin model descriptors of the MEP are used, the NF-κB model contains descriptors of the HBP. Both types of descriptors are not interchangeable, as then models with low clustering and a high number of conflicts are obtained (results not shown). Molecular surface properties describe the interaction of a drug and its protein target necessary for initial docking of the compound to the protein. Both surface properties differ with respect to functional groups and the kind of interactions. MEP is associated with long-range electrostatic interactions[28] and is a valuable and often-used descriptor for QSAR investigations and drug design.[29] Nevertheless, there are examples that, similar to the NF-κB data set, hydrogen bonding descriptors yield a better differentiation of active and inactive substances than MEP descriptors as shown for an hydantoin-data set with antagonistic activity.[30]

Conclusion

A QSAR model for the serotonin release inhibition activity of sesquiterpene lactones based on counterpropagation neural networks could be developed using 3D structure descriptors of the atom properties π-electronegativity (χ_π) and σ-charge (q_σ), as well as of the molecular electrostatic potential projected on the molecular surface. Comparison of these descriptors with the ones used in the NF-κB inhibition model previously published[12] provided information on the structural prerequisites for both types of biological activity and enables selection of SLs with more specific activities. Whereas some descriptors (χ_π descriptors at atom distances of r = 1.4, 1.5, 4.4, 4.5 Å) describe the structural requirements for both types of activities, other descriptors can be used to decide whether a sesquiterpene lactone is more active to NF-κB (χ_π descriptors at atom distances of r = 2.6, 3.5 Å; descriptors based on the hydrogen bonding potential) or to serotonin release (descriptors based on the MEP). This model has also the advantage to exclude structural features relevant for cytotoxic activities when looking for serotonin release inhibitors. This study shows that the descriptors used here, accessible with ADRIANA-Code,[24] have a clear structural and physicochemical basis that makes them amenable to interpretation and allows the development of structural models for biological activity. Furthermore, it is shown that a counterpropagation neural network is a valuabe tool in the development of more specific lead structures.

Experimental Section

Data Set. The SLs of the data set are listed in Table 7, and the structures are shown in Figure 6. The biological activities are published in Marles et al.[6] The activities were expressed as classes between 1 and 6 (1, $IC_{50} < 5\ \mu M$; 2, $5\ \mu M \le IC_{50} < 10\ \mu M$; 3, $10\ \mu M \le IC_{50} < 40\ \mu M$; 4, $40\ \mu M \le IC_{50} < 100\ \mu M$; 5, $100\ \mu M \le IC_{50} < 300\ \mu M$; 6, $300\ \mu M \le IC_{50}$). The serotonin release inhibition was determined by monitoring the serotonin release from bovine platelets. Therefore, cattle venous blood was treated with [^{14}C]-serotonin, which was taken up into the platelets by active transport. A platelet-rich plasma with a standard concentration of platelets was prepared by centrifugation and dilution. The platelet-rich plasma was preincubated with the different SLs, and then adenosine diphosphate was added to stimulate platelet aggregation and degranulation. After 6 min the reaction was stopped using ice-cold acetylsalicylic acid. After centrifugation the supernatant was subjected to scintillation counting.[31]

Structure Representations. Single low-energy 3D conformations were generated by CORINA.[32] Most of the SLs used show a rigid ring system (eudesmanolides, guaianolides, pseudoguaianolides, and some germacranolides). The remaining germacranolides possess a more flexible ring system, but the flexibility is also limited by double bonds, epoxide rings, and lactone rings.[33] Furthermore, RDF descriptors often remain unaffected by changes of the conformation. Therefore, one single conformation was regarded as sufficient. On the basis of the 3D conformation, four global molecular properties, seven physiochemical atomic properties, and three surface potentials were calculated (Table 1). ANN needs a vectorial representation with a fixed number of entries per molecule. To obtain such a representation for the atomic properties and surface potentials, a mathematical transformation is necessary. This was achieved for the atomic properties by using the RDF code. For an ensemble of atoms, the RDF code can be simplifiedly interpreted as the probability distribution of the individual interatomic distances r regarding the respective atomic properties:

$$g(r) = \sum_{i=1}^{N-1} \sum_{j>i}^{N} p_i p_j e^{-B(r - r_{ij})^2} \quad (1)$$

where p_i and p_j are the atomic properties of atoms i and j, N is the number of atoms within the molecule, r_{ij} the distance between atoms i and j, and B is a smoothing factor.[34,35]

The surface potentials were transformed by the RDF-like autocorrelation coefficients (AC, eqs 2 and 3):[36]

$$A(d_l, d_u) = \sum_{i=1}^{N} \sum_{j=i}^{N} \delta(d_{ij}, d_l, d_u) p_j p_i \quad (2)$$

$$\delta(d_{ij}, d_l, d_u) = \begin{cases} 1 \forall\, d_l < d_{ij} \le d_u \\ 0 \forall\, d_{ij} \le dl \vee d_{ij} > d_u \end{cases} \quad (3)$$

Here, the products of property p for surface point i and j possessing an Euclidian distance d within the boundaries d_l (lower) and d_u(upper) were summarized. Both representations are uniform and invariant under translation and rotations of the molecule. They were calculated using a sampling rate of 0.1 Å, a vector dimension of 128 and an interval of 0.0−12.8 Å. All the calculations were done by ADRIANA.code.[24]

Reduction of the Number of Descriptors and Preprocessing. For each atomic property and surface potential a vector with 128 descriptors was obtained, respectively. From these data sets, descriptors with constant values for all molecules were excluded. Furthermore, means and standard deviation of a descriptor within each activity class were calculated and compared using a statistical t test. Only those descriptors were selected by which the activity classes could be partially differentiated ($t > 2$). The selected descriptors of each data set were tested for linear independence. All selected and linearly independent descriptors of one data set were combined to a new data set including between 6 and 15 descriptors (Table 1).

All descriptors of the reduced vectors and the four global molecular descriptors were normalized between 0 and 1 using a range scaling procedure:[37]

$$x_{\text{new},i} = \frac{x_i - \min(x)}{\max(x) - \min(x)} \quad (4)$$

Generation of Self-Organizing Network. Generation of the Kohonen networks and the CPGNN was done by SONNIA (Self-Organizing Neural Network for Information Analysis).[38] Both ANNs consist of an n-dimensional input layer, where n is the number of the used descriptors. CPGNN also possess an output layer with the serotonin release inhibitory activity. This additional layer can be 1-dimensional with activity classes expressed as numbers from 1 to 6 or 6-dimensional using one output layer for each activity class (Figure 7).[19,20,39]

The Kohonen networks were used to search for properties and combinations thereof important for the inhibitory activity on serotonin release of SLs. Training of a Kohonen network started with initializing the neurons. Then a vector (a molecule) of input variables is presented to all neurons. The neuron was selected that had weights being closest to the input variables. The weights of this so-called winning neuron as well as the weights of neurons in the neighborhood were adjusted to the input vector. The degree of adaptation decreases with increasing distance to the winning neuron. The presentation and adaptation were done for each vector, that is, for each molecule. The whole process was iterated. After training, the response of the network was calculated for each vector of the data set. Subsequently, the projection of the data set into the 2-dimensional space was performed by mapping the activity of each vector into the coordinates of its winning neuron. CPGNN were used for validation and prediction. The training process was similar to that one of the Kohonen network, but the weights of the output layer were also adapted. The results were visualized as 2-dimensional maps by looking at the output map and identifying each molecule by its class assignment (e.g., Figure 2).

For both ANNs different sizes were tested. The clustering ability was evaluated by the same quality criteria as described in the next paragraph. A size of $5 \times 10 \times n$ turned out to be the best. This size was used throughout the study. In order to allow a direct comparison of all experiments, the topology of both ANNs was toroidal and the same training parameters were used.[40]

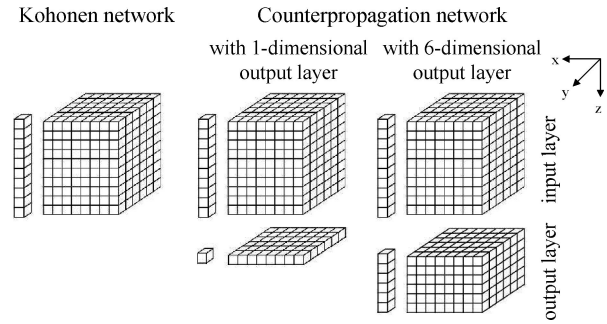

Figure 7. Architecture of the used neural networks and the associated data vectors. Kohonen networks (left) consist only of an input layer. By contrast, CPGNN possess an additional output layer containing the information of the serotonin release inhibition that is classified in six classes. Encoding the activity as natural numbers between 1 and 6, a 1-dimensional output layer is used. Furthermore, the activity classes can be binary coded yielding a 6-dimensional output layer whereby each layer refers to one activity class.

Search for Good Clustering Properties. Kohonen networks were trained with each data set. The resulting output maps were evaluated according to their clustering abilities. After a visual evaluation of the maps, correct clustering, occupancy, and conflicts were calculated. A neuron was classified as correctly clustered when neurons with the same inhibitory activity dominated in neighboring neurons. Conflicts occur when molecules with different inhibitory activity were put in the same neuron. Neurons including SLs with neighboring activity classes were not regarded as conflicts. Analogously, decision was done whether the predicted class of a SL was correct or not in the validation process.

Validation. A 10-fold cross-validation (CV) was performed for the best model using CPGNN with a 6-dimensional output layer (Figure 7).[41] The data set was divided by random splitting into 10 subsets. Nine subsets build the training set, and the remaining set was used as test set. Nineteen CPGNNs were calculated on the basis of the training set using random seeds for initialization. The procedure was repeated until each subset had been used as test set. Then a new splitting was performed, and the whole procedure was repeated. Altogether, 19 random splittings were carried out. Consequently, 3610 ($10 \times 19 \times 19$) CPGNN simulations using 5×10 rectangular topography were the basis for one 10-fold CV.

References

(1) Schmidt, T. J. Toxic activities of sesquiterpene lactones: structural and biochemical aspects. *Curr. Org. Chem.* **1999**, *3*, 577–608.

(2) Zhang, S.; Won, Y. K.; Ong, C. N.; Shen, H. M. Anti-cancer potential of sesquiterpene lactones: bioactivity and molecular mechanisms. *Curr. Med. Chem. Anti-Cancer Agents* **2005**, *5*, 239–249.

(3) Garcia-Pineres, A. J.; Castro, V.; Mora, G.; Schmidt, T. J.; Strunck, E.; Pahl, H. L.; Merfort, I. Cysteine 38 in p65/NF-kappaB plays a crucial role in DNA binding inhibition by sesquiterpene lactones. *J. Biol. Chem.* **2001**, *276*, 39713–39720.

(4) Hehner, S. P.; Heinrich, M.; Bork, P. M.; Vogt, M.; Ratter, F.; Lehmann, V.; Schulze-Osthoff, K.; Droge, W.; Schmitz, M. L. Sesquiterpene lactones specifically inhibit activation of NF-kappa B by preventing the degradation of I kappa B-alpha and I kappa B-beta. *J. Biol. Chem.* **1998**, *273*, 1288–1297.

(5) Lyss, G.; Knorre, A.; Schmidt, T. J.; Pahl, H. L.; Merfort, I. The anti-inflammatory sesquiterpene lactone helenalin inhibits the transcription factor NF-kappaB by directly targeting p65. *J. Biol. Chem.* **1998**, *273*, 33508–33516.

(6) Marles, R. J.; Pazos-Sanou, L.; Compadre, C. M.; Pezzuto, J. M.; Bloszyk, E.; Arnason, J. T. Sesquiterpene lactones revisited. In

Phytochemistry of Medicinal Plants; Arnason, J. T., Ed.; Plenum Press: New York, 1995; pp 333–356.
(7) Haefner, B. The transcription factor NF-kappaB as drug target. *Prog. Med. Chem.* **2005**, *43*, 137–188.
(8) Krakauer, T. Molecular therapeutic targets in inflammation: cyclooxygenase and NF-κB. *Curr. Drug Targets* **2004**, *3*, 317–324.
(9) Nakanishi, C.; Toi, M. Nuclear factor-kB inhibitors as sensitizers to anticancer drugs. *Nat. Rev. Cancer* **2005**, *5*, 297–309.
(10) Pande, V.; Ramos, M. J. NF-kappaB in human disease: current inhibitors and prospects for de novo structure based design of inhibitors. *Curr. Med. Chem.* **2005**, *12*, 357–374.
(11) Merfort, I. Patented inhibitors (2002–2005) of the transcription factor NF-kappaB. *Expert Opin. Ther. Pat.* **2006**, *16*, 1–14.
(12) Wagner, S.; Hofmann, A.; Siedle, B.; Terfloth, L.; Merfort, I.; Gasteiger, J. Development of a structural model for NF-kappaB inhibition of sesquiterpene lactones using self-organizing neural networks. *J. Med. Chem.* **2006**, *49*, 2241–2252.
(13) Silberstein, S. D.; Goadsby, P. J. Migraine: preventive treatment. *Cephalalgia* **2002**, *22*, 491–512.
(14) Diener, H. C.; Pfaffenrath, V.; Schnitker, J.; Friede, M.; Henneicke-von Zepelin, H. H. Efficacy and safety of 6.25 mg t.i.d. feverfew CO2-extract (MIG-99) in migraine prevention−a randomized, double-blind, multicentre, placebo-controlled study. *Cephalalgia* **2005**, *25*, 1031–1041.
(15) Groenewegen, W. A.; Knight, D. W.; Heptinstall, S. Compounds extracted from feverfew that have anti-secretory activity contain an alpha-methylene butyrolactone unit. *J. Pharm. Pharmacol.* **1986**, *38*, 709–712.
(16) Schroder, H.; Losche, W.; Strobach, H.; Leven, W.; Willuhn, G.; Till, U.; Schror, K. Helenalin and 11 alpha,13-dihydrohelenalin, two constituents from Arnica montana L., inhibit human platelet function via thiol-dependent pathways. *Thromb. Res.* **1990**, *57*, 839–845.
(17) Schmidt, T. J. Helenanolide-type sesquiterpene lactones. III. Rates and stereochemistry in the reaction of helenalin and related helenanolides with sulfhydryl containing biomolecules. *Bioorg. Med. Chem.* **1997**, *5*, 645–653.
(18) Garcia-Pineres, A. J.; Lindenmeyer, M. T.; Merfort, I. Role of cysteine residues of p65/NF-kappaB on the inhibition by the sesquiterpene lactone parthenolide and N-ethyl maleimide, and on its transactivating potential. *Life Sci.* **2004**, *75*, 841–856.
(19) Zupan, J.; Gasteiger, J. *Neural Networks in Chemistry and Drug Design*; Wiley-VCH: Weinheim, 1999.
(20) Kohonen, T. Self-organized formation of topologically correct feature maps. *Biol. Cybern.* **1982**, *43*, 59–69.
(21) Kohonen, T. Analysis of a simple self-organizing process. *Biol. Cybern.* **1982**, *44*, 135–140.
(22) Guha, R.; Serra, J. R.; Jurs, P. C. Generation of QSAR sets with a self-organizing map. *J. Mol. Graph. Model.* **2004**, *23*, 1–14.
(23) Lindenmeyer, M. T.; Hrenn, A.; Kern, C.; Castro, V.; Murillo, R.; Muller, S.; Laufer, S.; Schulte-Monting, J.; Siedle, B.; Merfort, I. Sesquiterpene lactones as inhibitors of IL-8 expression in HeLa cells. *Bioorg. Med. Chem.* **2006**, *14*, 2487–2497.
(24) Descriptor calculation package ADRIANA.Code is available from Molecular Networks GmbH, Erlangen, Germany (http://www.molecular-networks.com, accessed January, 2008).
(25) Siedle, B.; Garcia-Pineres, A. J.; Murillo, R.; Schulte-Monting, J.; Castro, V.; Rungeler, P.; Klaas, C. A.; Da Costa, F. B.; Kisiel, W.; Merfort, I. Quantitative structure-activity relationship of sesquiterpene lactones as inhibitors of the transcription factor NF-kappaB. *J. Med. Chem.* **2004**, *47*, 6042–6054.
(26) Luo, Q.; Darsey, J. A.; Compadre, C. M.; Mitra, S. K. Prediction of potential antimigraine activity using artificial neural networks. *J. Arkansas Acad. Sci.* **1997**, *51*, 131–134.
(27) Kupchan, S. M.; Eakin, M. A.; Thomas, A. M. Tumor inhibitors. 69. Structure-cytotoxicity relationships among the sesquiterpene lactones. *J. Med. Chem.* **1971**, *14*, 1147–1152.
(28) Huang, X.; Zheng, F.; Chen, X.; Crooks, P. A.; Dwoskin, L. P.; Zhan, C. G. Modeling subtype-selective agonists binding with alpha4beta2 and alpha7 nicotinic acetylcholine receptors: effects of local binding and long-range electrostatic interactions. *J. Med. Chem.* **2006**, *49*, 7661–7674.
(29) Mezey, P. G. Molecular surfaces. In *Reviews in Computational Chemistry*; Lipkowitz, K. B., Boyd, D. B., Eds.; VCH Publisher: New York, Weinheim, Cambridge, 1990; pp 265–294.
(30) Teckentrup, A.; Briem, H.; Gasteiger, J. Mining high-throughput screening data of combinatorial libraries: Development of a filter to distinguish hits from nonhits. *J. Chem. Inf. Comput. Sci.* **2004**, *44*, 626–634.
(31) Marles, R. J.; Kaminski, J.; Arnason, J. T.; Pazos-Sanou, L.; Heptinstall, S.; Fischer, N. H.; Crompton, C. W.; Kindack, D. G.; Awang, D. V. A bioassay for inhibition of serotonin release from bovine platelets. *J. Nat. Prod.* **1992**, *55*, 1044–1056.
(32) 3D Structure Generator CORINA is available from Molecular Networks GmbH, Erlangen, Germany (http://www.molecular-networks.com, accessed January, 2008).
(33) Rungeler, P.; Brecht, V.; Tamayo-Castillo, G.; Merfort, I. Germacranolides from Mikania guaco. *Phytochemistry* **2001**, *56*, 475–489.
(34) Hemmer, M. C.; Steinhauer, V.; Gasteiger, J. Deriving the 3D structure of organic molecules from their infrared spectra. *Vib. Spectrosc.* **1999**, *19*, 151–164.
(35) Hemmer, M. C.; Gasteiger, J. Prediction of three-dimensional molecular structures using information from infrared spectra. *Anal. Chim. Acta* **2000**, *420*, 145–154.
(36) Gasteiger, J.; Engel, T. *Chemoinformatics: A Textbook*; Wiley-VCH: Weinheim, 2003.
(37) Mazzatorta, P.; Vracko, M.; Jezierska, A.; Benfenati, E. Modeling toxicity by using supervised Kohonen neural networks. *J. Chem. Inf. Comput. Sci.* **2003**, *43*, 485–492.
(38) Neural networks package SONNIA is available from Molecular Networks GmbH, Erlangen, Germany (http://www.molecular-networks.com, accessed January, 2008).
(39) Anzali, S.; Gasteiger, J.; Holzgrabe, U.; Polanski, J.; Sadowski, J.; Teckentrup, A.; Wagener, M. The use of self-organizing neural networks in drug design. In *3D QSAR in Drug Design*; Kubinyi, H., Folkers, G., Martin, Y. C., Eds.; Kluwer/ESCOM: Dordrecht, 1998; Vol. 2, pp 273–299.
(40) *SONNIA.User Manual*, Version 1.0; Molecular Networks GmbH: Erlangen, Germany. http://www.molecular-networks.com/software/sonnia/sonnia_manual.pdf, accessed January, 2008.
(41) Spycher, S.; Pellegrini, E.; Gasteiger, J. Use of structure descriptors to discriminate between modes of toxic action of phenols. *J. Chem. Inf. Model.* **2005**, *45*, 200–208.

JM701318X